ISSN: 2639-0108

Research Article

Advances in Theoretical & Computational Physics

Experimental Demonstration of an All-Optical NOT Logic Gate Based on Combined Brillouin Gain and Loss in an Optical Fiber

Daisy Williams*

Optii Corporation, D2-150 Terence Matthews Crescent, Ottawa, Ontario K2M 1X4 Canada

***Corresponding Author**
Daisy Williams, dwilliams@optii.ca.

Submitted: 2024, Sep 02; **Accepted:** 2024, Oct 29; **Published:** 2024, Nov 29

Citation: Williams, D. (2024). Experimental Demonstration of an All-Optical Not Logic Gate Based On Combined Brillouin Gain and Loss in an Optical Fiber. *Adv Theo Comp Phy, 7*(4), 01-05.

Abstract

An all-optical NOT logic gate, based on combined Brillouin gain and loss in an optical fiber, has been experimentally demonstrated. An input (IN) to the NOT gate is a probe wave, which is a combined Stokes and anti-Stokes wave, and the output (OUT) is a pump wave. The pump and probe waves undergo a combined Brillouin gain and loss interaction in an optical fiber of 20.56 km length, which enables the switching mechanism of the NOT gate. A switching contrast of 43-45% has been experimentally achieved, which is in line with previously published theoretical simulations of the NOT optical gate.

1. Introduction

All-optical logic gates have been the subject of recent research efforts into the development of integrated photonic circuits and switches [1-8]. Speed, compactness and efficiency have been the primary focus of efforts in the industry [6-8], however, few investigations have been made into techniques which minimize polarization-induced signal fluctuations that cause spectral distortions. In [1-5], all-optical NAND/NOT/AND/OR logic gates based on combined Brillouin gain and loss in an optical fiber have been theoretically simulated to show spectral stability in various circumstances. Like Brillouin sensors [9], all-optical logic gates based on Brillouin gain and loss have the required stability to operate in rugged military environments, where changes in temperature and strain, and vibrations are prominent. In the current paper, an experimental demonstration of an all-optical NOT logic gate [1-5] is presented.

2. Experimental Setup

An all-optical NOT gate based on a variation of the setup of [1-5] has been experimentally demonstrated in a single mode SMF-28e optical fiber of a 20.56 km length.

The schematic diagram of the NOT gate is shown in Fig. 1. The combined input Stokes and anti-Stokes waves $SW_{in}+ASW_{in}$ form the input probe wave with power P_{20} at one end of the fiber, which is the input of the NOT gate (IN). The input continuous pump wave CW_{in} with power P_{10} at the opposite end of the fiber, to be referred to as a reference signal (REF) of the NOT gate, is held constant. The output continuous pump wave CW_{out}, with power P_{1-out} at one end of the fiber, is the output of the NOT gate (OUT). In comparison with the theory of [1-5], in our experimental setup the probe wave is a combination of the Stokes and anti-Stokes waves $SW+ASW$.

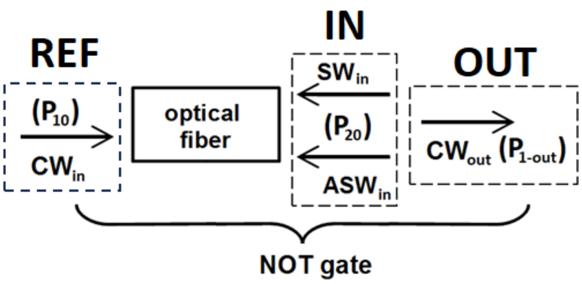

Figure 1: Schematic Diagram of the NOT Gate

In Fig. 1, the interaction of the pump and probe waves in the optical fiber, during the Brillouin gain and loss regime [1-5], enables the switching mechanism of the NOT gate via the energy transfer between the *CW, SW* and *ASW*. Namely, for certain power regimes, fiber lengths and parameters of the fiber [1-5], a low input probe wave power (IN) yields a high output pump wave power (OUT), and vice versa, thus enabling the switching between "0" and "1" of the NOT gate. This will be described in more detail in section 3 below.

The experimental setup of the NOT gate is shown in Fig. 2. The light from the Distributed Feedback Laser (DFB), operating at 1550 nm and output power of 2.05 mW, is split by a 50:50 splitter into the pump wave (*CW*), and another wave, which is passed through a first polarization controller. Then, the other wave is modulated by an electro-optic modulator (EOM) that is driven by a Radio Frequency (RF) source at 10.86 GHz and a voltage source V at 1.55 volts, to become the probe wave (*SW+ASW*). The first polarization controller adjusts the polarization of the *CW*, to maximize the contrast between the probe wave (*SW+ASW*) and the polarization-adjusted pump wave (*CW*).

The probe wave is amplified by an erbium-doped fiber amplifier (EDFA1) controlled by an electronic variable optical attenuator (eVOA).

The amplified probe wave from the EDFA1 is passed through a first circulator and is sent into one end of the fiber under test (FUT) of length of about 20.56 km, thus becoming the input of the NOT gate (IN).

The pump wave from the 50:50 splitter is sent directly to another EDFA2 for amplification, and then passed through a second polarization controller which is adjusted to maximize the power of the pump wave. The pump wave then passes through a second circulator and enters the opposite end of the FUT, becoming the reference signal (REF) with constant power P_{10}.

The P_{10} is measured by a power meter before it is sent into the FUT. After passing through the FUT and experiencing energy transfer during the combined Brillouin gain and loss process, the output pump wave passes through a second circulator and becomes the output of the NOT gate (OUT) with power $P_{1\text{-}out}$, which is measured by a power meter.

The powers of the pump wave (*CW*) and probe wave (*SW+ASW*) were measured with a JonardTools® optical power meter.

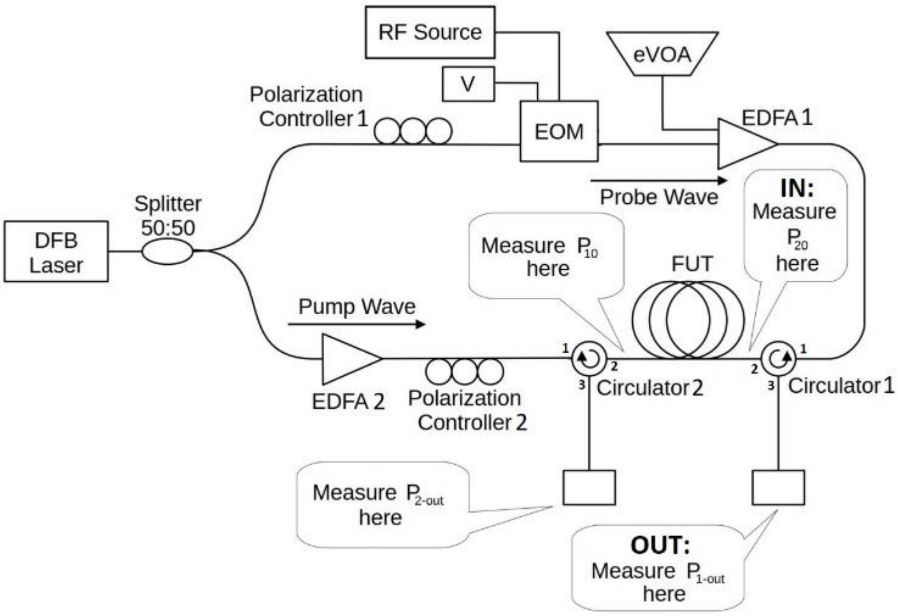

Figure 2: Experimental NOT Gate Configuration

Significant energy transfer between the pump, Stokes and anti-Stokes waves, during the combined Brillouin gain and loss regime, is the basis of the switching mechanism between the input IN and the output OUT of the NOT gate.

The output pump wave power $P_{1\text{-}out}$ is measured for different input probe wave powers P_{20}, to determine the switching contrast of the NOT gate, which will be described in more detail in section 3 below.

3. Experimental Results

The power of the probe wave is controlled by the eVOA, and the attenuation is measured in dB. The lowest probe wave attenuation (*LA*) of the eVOA was 2.5 dB, which yielded the highest probe wave power P_{20} = 1.4 mW. The probe wave attenuation was then increased in increments of 1 dB to a highest probe wave attenuation (*HA*) of 19.5 dB, which yielded the lowest probe wave power P_{20} = 30 µW.

The switching contrast of the NOT gate is defined as the percentage change of the output pump wave power, between the lowest probe wave attenuation (*LA*), $P_{1\text{-}out(LA)}$ (yielding the highest probe wave power), and the highest probe wave attenuation (*HA*), $P_{1\text{-}out(HA)}$ (yielding the lowest probe wave power), and is calculated as follows:

$$Switching\ Contrast = [P_{1\text{-}out\ (HA)} - P_{1\text{-}out\ (LA)}]/P_{1\text{-}out\ (HA)} \cdot 100\% \quad (1)$$

Fig. 3 shows experimental results of the output pump wave power, $P_{1\text{-}out}$, versus the attenuation of the probe wave over the course of 5 independent trials. The power of the reference signal (REF) was held constant at P_{10} = 7.8 mW. As mentioned above, the initial input signal of the NOT gate (IN) was taken to be P_{20} = 1.4 mW, corresponding to an attenuation of 2.5 dB, and measurements of $P_{1\text{-}out}$ were taken at increments corresponding to gradual attenuation increases of 1 dB.

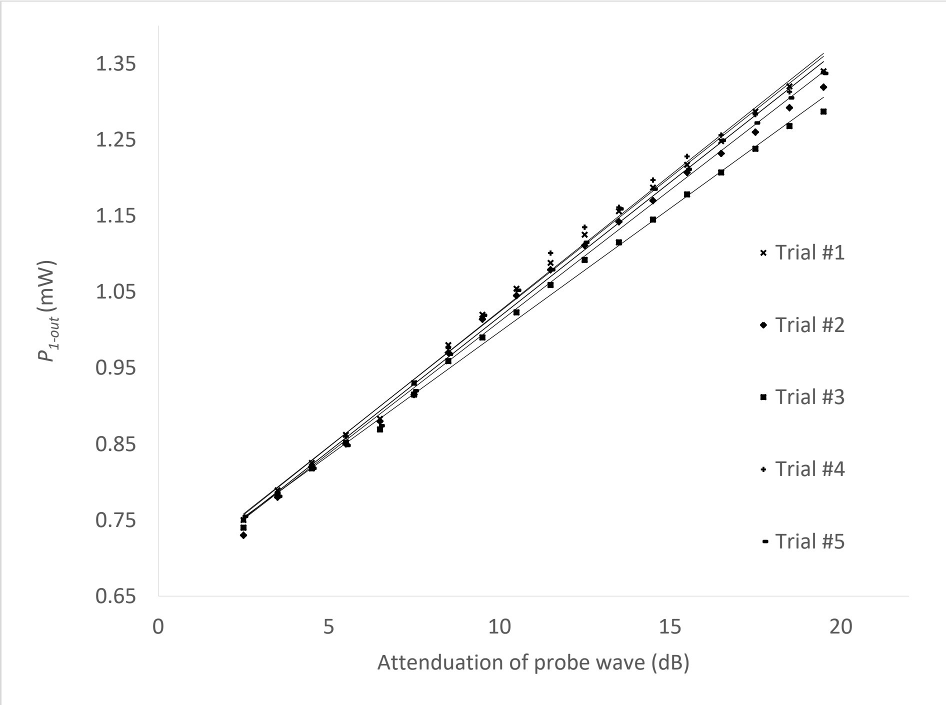

Figure 3: Output Pump Power vs. Probe Wave Attenuation

In each trial, the following measurements were made as shown in Table 1 below, resulting in the corresponding switching contrasts according to equation (1) above:

Trial #	**$P_{1\text{-}out(LA)}$ (mW)**	**$P_{1\text{-}out(HA)}$ (mW)**	**Switching Contrast (%)**
1	0.75	1.34	44
2	0.73	1.32	45
3	0.74	1.29	43
4	0.75	1.34	44
5	0.76	1.34	44

Table 1: Switching Contrast of NOT Gate for Trials #1-5 (Fig. 3)

In Fig. 3, the measurements at the lower-left area of the graph, corresponding to low attenuations of the probe wave, are limited by noise in the fiber, while at the upper-right area of the graph, corresponding to high attenuations of the probe wave, are limited by the disappearance of Brillouin scattering. At the high limit of probe wave attenuation beyond 19.5 dB, the probe wave is attenuated to near zero, and Brillouin scattering will no longer occur.

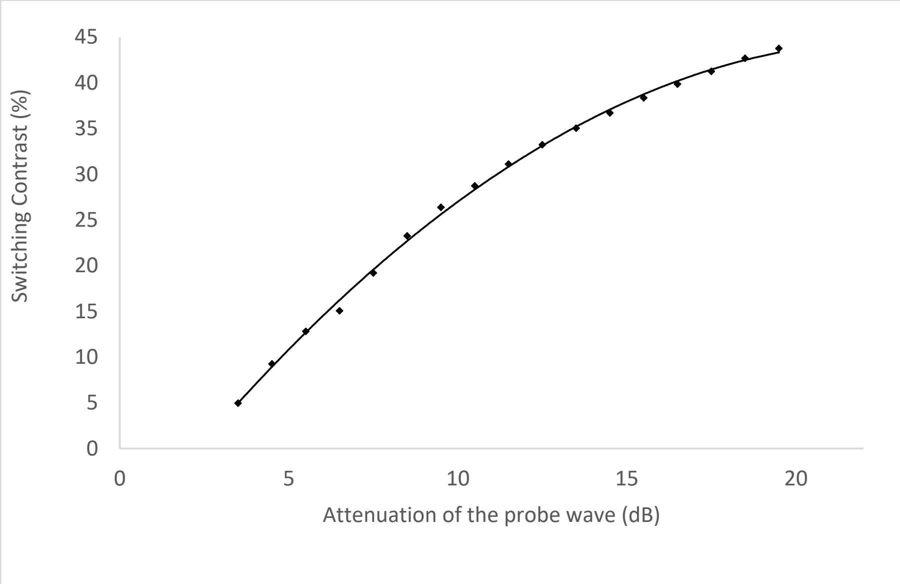

Figure 4: Switching Contrast vs. Probe Wave Attenuation for $P_{1\text{-}out(LA)}$ at 2.5 dB

Fig. 4 shows the dependence of the switching contrast on the attenuation of the probe wave for $P_{1\text{-}out(LA)}$ at 2.5 dB. Experimental results of $P_{1\text{-}out}$ have been averaged over the five trials of Fig. 3. $P_{1\text{-}out(LA)}$ was held constant, corresponding to an attenuation of 2.5 dB. Then, $P_{1\text{-}out(HA)}$ was progressively assigned values of $P_{1\text{-}out}$ corresponding to attenuations between 3.5 to 19.5 dB, in 1 dB increments. For each increment, the switching contrast was determined according to equation (1). As shown in Fig. 4, the higher the attenuation of the probe wave, the higher is the resulting switching contrast of the NOT gate.

4. Discussion

The underlying switching mechanism of the NOT gate is a result of energy transfer between the pump, Stokes and anti-Stokes waves during the combined Brillouin gain and loss regime.

In the combined Brillouin gain and loss regime, energy is transferred from higher frequency waves to lower frequency waves – the *ASW* transfers energy to the *CW*, which in turn transfers energy to the *SW*.

The relative strength between the pump and probe wave powers, and the direction of the energy transfer between the *CW, SW* and *ASW*, enable the control of the output pump wave power, $P_{1\text{-}out}$, via the input power of the probe wave P_{20}.

The NOT gate is achieved by using different Brillouin gain and loss power regimes. A balanced pump-probe power arrangement will yield a high gain/loss Brillouin regime, resulting in a higher overall pump depletion [9,10]. In contrast, if the relative strength between the pump and probe waves is imbalanced, with a significantly stronger pump wave as compared to the probe wave (*SW*+*ASW*), this yields a low gain/loss Brillouin regime, and in extreme cases, a constant-pump approximation may be used to describe this regime [10].

Fig. 5 illustrates the frequency and power relationship between the *CW, SW* and *ASW* during different combined Brillouin gain and loss regimes, and the resulting operation of the NOT gate. Referring to Fig. 5(a), the input probe wave power, P_{20}, is chosen to be comparable with the pump wave power at the input of the FUT. In our experiment, the initial power of the probe wave was chosen to be P_{20} = 1.4 mW, which is comparable to the input power of the pump wave (P_{10} = 7.8 mW). Hence, a high gain/loss Brillouin regime is initiated. The input of the NOT gate (P_{20}) is relatively high, and is designated as “1” (IN). Referring to Fig. 5(b), because of the high gain/loss SBS regime, there is significant energy transfer between the *CW*, *SW* and *ASW*, and the output pump wave is significantly depleted. Hence the output of the NOT gate ($P_{1\text{-}out}$) is relatively low, and is designated as “0” (OUT).

Referring now to Fig. 5(c), as the attenuation of the probe wave is increased, the input probe wave is respectively decreased to about P_{20} = 30 μW, which is significantly lower than the input pump wave power (P_{10} = 7.8 mW). The disparity between the pump and probe wave powers is increased, hence, a low gain/loss Brillouin regime is initiated. This interaction may be described by a constant-pump approximation.

Referring to Fig. 5(c), the input of the NOT gate (P_{20}) is significantly low, and is designated as “0” (IN). Because of the low gain/loss Brillouin regime, there is little energy transfer (if any) between the *CW, SW* and *ASW*, and the output pump wave power remains significantly constant, as shown in Fig. 5(d). Hence, the output of the NOT gate ($P_{1\text{-}out}$) remains relatively high, and is designated as “1” (OUT).

Comparing Fig. 5(a), 5(b) and 5(c), 5(d), the pump wave is depleted significantly when paired with a stronger probe wave during the high gain/loss regime, as compared with a weaker probe wave in the low gain/loss regime. Hence, when the probe wave is significantly attenuated and the pump wave approaches a constant-pump regime, the change in output power between the previously-depleted pump at the high gain/loss regime, and the un-depleted (near-constant) pump, becomes significant. Namely, the result is an *apparent* increase in the power of the output pump wave, as the power of the probe wave is increasingly attenuated.

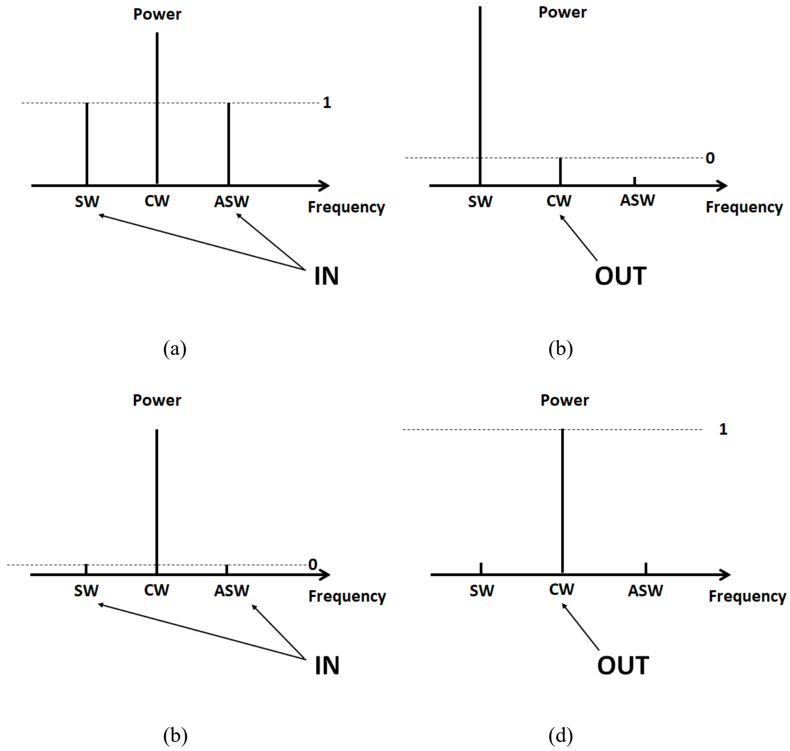

Figure 5: Operation of NOT Gate via Brillouin Gain/Loss
(a),(b) High Gain/Loss Regime; (c),(d) Low Gain/Loss Regime

5. Conclusion

An all-optical NOT logic gate, based on the principles of combined Brillouin gain and loss in an optical fiber, has been experimentally demonstrated. Consistent switching contrasts of the NOT gate between 43-45% have been achieved, which is in good correspondence with the theoretical predictions of [1-5], and their stability is sufficient for practical applications. Future experimental work will aim at expanding the range of logical gates, and finding optimized conditions of operation for military and commercial applications.

References

1. Williams, D., Bao, X., & Chen, L. (2013). All-optical NAND/NOT/AND/OR logic gates based on combined Brillouin gain and loss in an optical fiber. *Applied Optics, 52*(14), 3404-3411.
2. Williams, D., Bao, X., & Chen, L. (2014). Improved all-optical OR logic gate based on combined Brillouin gain and loss in an optical fiber. *Chinese Optics Letters, 12*(8), 082001.
3. Williams, D., Bao, X., & Chen, L. (2016). *U.S. Patent No. 9,335,607.* Washington, DC: U.S. Patent and Trademark Office.
4. Williams, D., Bao, X., & Chen, L. (2017). All-optical NAND/NOT/AND/OR logic gates based on combined Brillouin gain and loss in an optical fiber. Canadian Patent 2,829,175.
5. Williams, D. (2014). Theoretical Investigation of stimulated Brillouin scattering in Optical Fibers and their Applications (Doctoral dissertation, Université d'Ottawa/University of Ottawa).
6. Anagha, E. G., & Jeyachitra, R. K. (2022). Review on all-optical logic gates: design techniques and classifications–heading toward high-speed optical integrated circuits. *Optical engineering, 61*(6), 060902-060902.
7. Agarwal, V., Agarwal, M., Pareek, P., Chaurasia, V., & Pandey, S. K. (2019). Ultrafast optical message encryption–decryption system using semiconductor optical amplifier based XOR logic gate. *Optical and Quantum Electronics, 51*(7), 221.
8. Hui, S., Wang, D., Wang, J., Yan, X., Li, Y., & Li, Z. (2023). A new scheme to implement the reconfigurable optical logic gate in Millimeter Wave over fiber system. *IEEE Access, 11,* 25835-25842.
9. Bao, X., & Chen, L. (2011). Recent progress in Brillouin scattering based fiber sensors. *Sensors, 11*(4), 4152-4187.
10. Chen, L., & Bao, X. (1998). Analytical and numerical solutions for steady state stimulated Brillouin scattering in a single-mode fiber. *Optics Communications, 152*(1-3), 65-70.